ENERGY EXPENDITURE AND LIMITATIONS IN SHOCK CONSOLIDATION

M. A. Meyers, D. J. Benson, and S. S. Shang
University of California, San Diego
La Jolla, California, 92093-0411

The energy dissipated by a shock wave as it traverses a powder is assessed. The various energy dissipation processes are analyzed: plastic deformation, interparticle friction, microkinetic energy, defect generation. An expression is developed for the energy requirement to shock consolidate a powder as a function of strength, size, porosity, and temperature, based on a prescribed interparticle melting layer. The corresponding pressures are calculated and it is shown that the activation of flaws occurs at tensile reflected pulses that are a decreasing fraction of the compressive pulse as the powder strength increases. These analytical results are compared to numerical solutions obtained by modeling the compaction of a discrete set of particles with an Eulerian finite element program.

INTRODUCTION

It is very important to estimate the total energy needed to consolidate a material and to determine the shock parameters required to effect such a consolidation by shock waves. This predictive capability has been obtained, for soft materials, through the energy flux models of Gourdin [1] and Schwarz *et al.* [2]. For harder materials, the energy expended in plastic deformation becomes an important component of the overall equation and energy predictions incorporating plastic work have been made by Nesterenko [3] and Ferreira and Meyers [4].

A model for the total energy requirement is developed and applied to some typical "hard" materials: SiC, c-BN, diamond, and Ti_3Al. This estimate of the overall energy enables us to establish the minimum shock energy required for consolidating powders as well as the energy partitioning, when other sources of energy other than shock energy are used. Additionally, the results of the large-scale Eulerian computations using a two-dimensional geometry (cylindrical particles) is presented. The calculational procedure developed by Benson [5] is an extension of the work of Williamson [6] and uses an Eulerian Finite Element Code well suited for the large plastic deformations ocurring in shock consolidation.

Figure 1 shows schematically the various phenomena occurring during shock compaction.These are: (a) The material is plastically deformed; the collapse of the voids requires plastic flow. A plastic deformation energy has to be computed. (b) The plastic flow

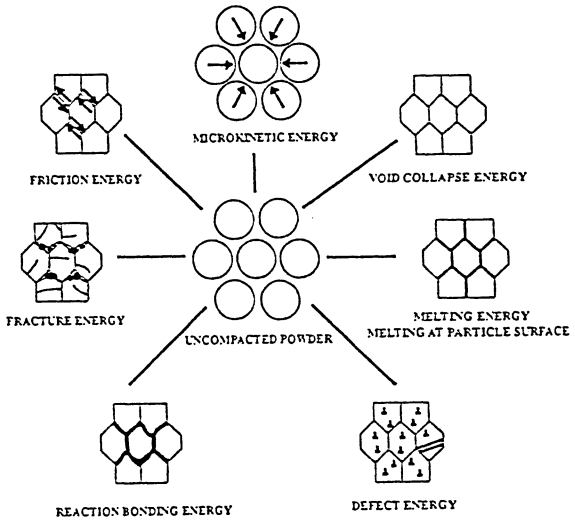

Figure 1. Schematic representation of energy dissipation processes in shock consolidation.

of the material is a dynamic process, leading to interparticle impact, friction, and plastic flow beyond the flow geometrically necessary to collapse the voids. We will call this component "microkinetic energy". The entire plastic deformation path is changed by virtue of the dynamics of the process. The kinetic energy acquired by the material elements being plastically deformed eventually dissipates into thermal energy. (c) Melting at interparticle regions: It is known that energy is preferentially deposited at the particle surface, leading eventually to their melting. This is the main

component of Schwarz *et al.* [2]. (d) Defect energy: Point, line, and interfacial defects are produced by the passage of the shock wave. (e) Friction energy: The rearrangement of the powders at the shock front requires relative motions, under the applied stress. Thus, friction may play a role in energy deposition at the shock front. (f) Fracture energy: Brittle materials may consolidate by fracturing. The comminuted particles can more efficiently fill the voids. (g) Gas compression: Compaction is most often conducted with the powder being initially at atmospheric pressure. Thus, the gaps between the powders are filled with gas. Shock compaction of the powders compresses and heats these gases. This effect was considered first by Lotrich, Akashi, and Sawaoka [7]. (h) Shock initiated chemical reactions: Reactive elements or compounds can be added to the powders that are being consolidated. These exothermic reactions can be used to deposit additional energy at the powder surfaces, thereby assisting bonding. This approach was introduced by Akashi and Sawaoka [8].

The eight "components" of the processes occurring during the passage of a shock wave through a granular medium described above and presented schematically in Figure 1 are not independent and there is some overlap. This is not a rigorous classification and should only be construed as a simplified explanation.

A primary purpose of the model presented herein is to incorporate the particle strength, which is identified as an important mechanism during densification of hard materials such as diamond, c-BN and SiC. For the sake of simplicity, this model considers only the spherical monosize particles and constrains all particles to deform in a uniform manner.

SIMPLE ANALYTICAL COMPUTATION OF SHOCK COMPACTION ENERGY REQUIREMENTS

The computation of the various components is presented in detail by Shang [9] and only the final expressions are given here.

Void Collapse Energy at Microscopic Level: One of the models that predict the pressure in porous materials as a function of density is the one by Helle *et al* [10]. The pressure is given by:

$$P_y = 2.97\ \rho^2 \frac{(\rho - \rho_0)}{(1 - \rho_0)} Y_y$$

Y_y is the flow stress of the material. The total energy required to densify the material is given by

$$E_{vc} = \frac{2.97\ Y_y}{1 - \rho_0}\left[\frac{(-\rho_f^2 - \rho_0^2)}{2} + \rho_f \rho_0\right]$$

Microkinetic Energy: Nesterenko [3] developed a model which describes the relative movement of particles under dynamic compression, as shown in Figure 2. Nesterenko's [3] modification of the Carroll-Holt model enables the introduction of a size scale and the separation of the plastic deformation process into two components, one of which has a substantial microkinetic energy. The external shell is directly responsible for the microkinetic energy, since it impacts the internal core, which is considered to be stationary. The impact velocity is given by $V=(a_0-c)/t$, and the microkinetic energy is given as

$$E_k = \frac{1}{2} m V^2 = \frac{1}{2} m \left(\frac{a_0 - c}{t}\right)^2$$

where m is the mass of the external shell.

Frictional Energy: The calculation of frictional energy is based on a pyramidal coordination and one-dimensional strain. This leads to:

$$E_f = \frac{0.1\ P\ \xi\ Z\ \mu}{\rho}$$

where μ is friction coefficient, P the applied stress, ρ the density, ξ fraction of contact surface, and Z the coordination number of the powders.

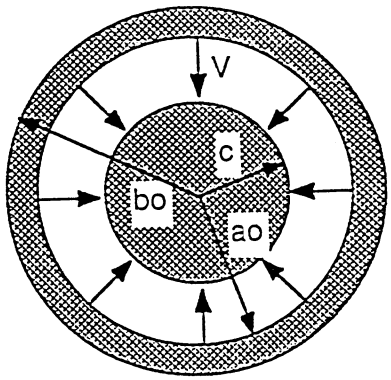

Figure 2. Nesterenko's [3] void collapse model.

Computation of the total Energy: The following problem is posed: what pressure is required to shock consolidate a specific material, if interparticle melting with a prescribed thickness is needed for good bonding between particles? The shock pressure can be estimated by equating the total shock energy with the sum of the void collapse, defect, microkinetic, and frictional energy, leading to:

$$P = \frac{2\rho_0\rho}{(\rho - \rho_0)}\left[\frac{1_m}{2}\left(\frac{a_0 - c}{t}\right)^2 + \frac{0.1\, P\, \xi\, Z\, \mu}{\rho} + \frac{2.97 Y_y}{1 - \rho_0}\left(\frac{-\rho_f^2 - \rho_0^2}{2} + \rho_f\rho_0\right)\right]$$

The defect energy (which is found to be negligible) is a component of the plastic deformation energy. The melting energy is a direct result of the plastic deformation, microkinetic, and friction energies. By considering a prescribed interparticle melting layer, it is possible to calculate the pressure required to consolidate a material as a function of initial density (distention) and particle size. This is shown in Figure 3 for SiC. A normalized plot of P/Y versus distention was produced for different particle sizes. As the distention increases, the P/Y ratio required for shock consolidation of a fixed particle size decreases. Conversely, as the particle size is decreased, the P/Y ratio required increases.

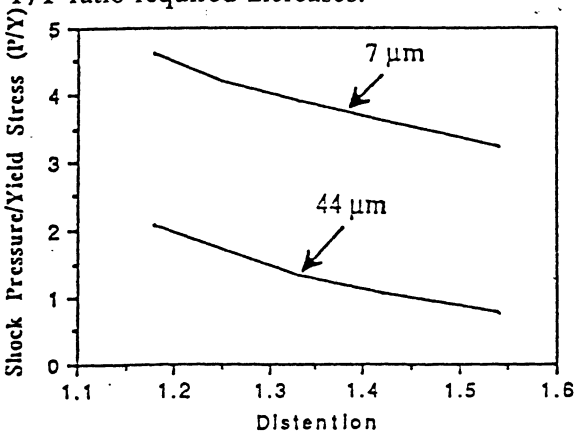

Figure 3. Computed pressure required for shock consolidation of SiC.

DIRECT NUMERICAL SIMULATION OF SHOCK COMPACTION

The complex deformation pattern occurring in shock consolidation is best captured by computational modeling. The simplifying assumptions in the simple analytical model presented in the previous section are very drastic and the physical processes are only brought out by numerical methods. Benson [11] presents an overview of explicit Lagrangian and Eulerian codes. A model boundary value problem was used to simulate the propagation of the shock wave through the powder. The tridimensional problem is reduced to two dimensions, and spherical particles (of varying diameters) are simulated as cylinders. The green density was taken as 80% of the theoretical density, and calculations were performed for copper and silicon carbide. The Steinberg-Guinan plasticity model [12] was used in combination with the Mie-Gruneisen equation of state. A particle size distribution was assumed based on experimental measurements. Figure 4(a) shows the original configuration of the powders, whereas the configurations after shock impact velocities of 0.25, 1, and 2 km/s on copper powder are shown in Figure 4(b). At 0.25 km/s the shock energy is sufficient to collapse all voids. As the impact velocity is increased, the "microkinetic" energy of the powders increases, and plastic deformation at the interfaces exceeds significantly the value needed for void collapse. Thus, one can separate this plastic deformation into a "geometrically necessary" component and a "redundant" component; the latter is due to the microkinetic energy and is responsible for the localized temperature spikes that lead to melting and bonding. Figure 5 shows the temperature profiles for the 1 km/s impact velocity. The melting point of copper is equal to 1355 K (P=1 atm) and it is clear that it is exceeded at the particle boundaries. Thus, the Eulerian Finite Element code correctly predicts the plastic deformation and interparticle melting. The application of the same calculational procedure to silicon carbide yields, at 1 km/s, results that are considerably different. This can be seen by comparing Fig. 4(b) and Figure 6. At 1 km/s, the shock energy is only sufficient to collapse the voids in SiC, whereas for copper a considerable amount of "redundant" plastic deformation takes place.

LIMITATIONS OF SHOCK CONSOLIDATION PROCESS

There exist two major problems in shock consolidation. One is cracking of the compacts at both the microscopic and macroscopic levels.

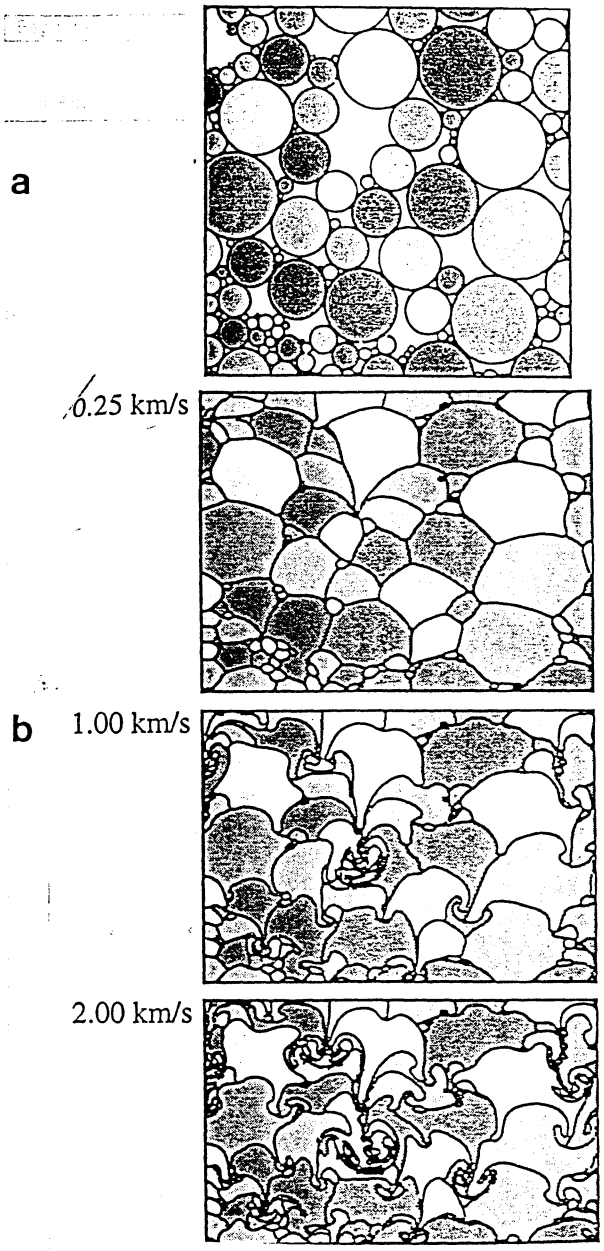

Figure 4. (a) Powder configuration for computational modeling; (b) configuration of consolidated Cu powders after impacts at different velocities (0.25, 1, and 2 km/s).

The other is a lack of uniformity in microstructure and mechanical properties within the resulting compacts. Figure 7(a) shows plots of critical flaw size, a, as a function of tensile stress, σ, for materials having different fracture toughnesses, K_{IC}. These plots were made using the well known fracture mechanics equation: $\sigma =$

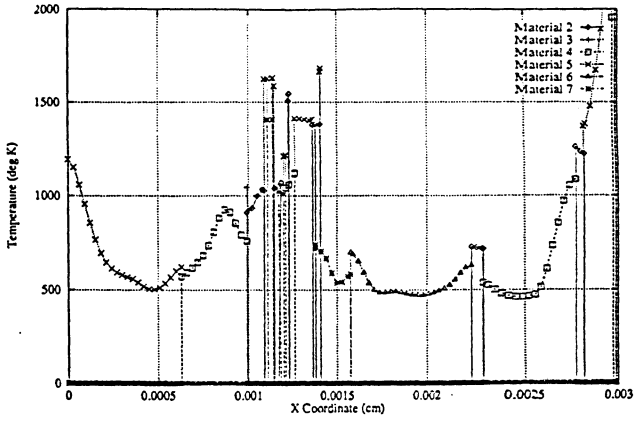

Figure 5. Temperature profile for copper impacted at 1 km/s.

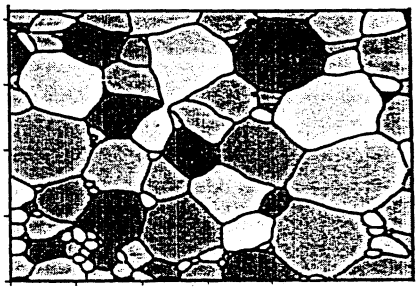

Figure 6. Configuration of consolidated SiC powders after 1 km/s impact velocity.

$K_{IC}/\sqrt{\pi a}$. It is difficult to conceive a shock consolidation process in which no flaws are left, and the particle size is a good indicator of the inherent flaw size in a shock consolidated material. The three fracture toughnesses given, 5, 50, and 100 MPa $\sqrt{m}$, are characteristic of brittle (ceramics), tough (steel, titanium alloys) and very ductile materials (copper, nickel), respectively. Figure 7(b) shows the critical tensile stresses for 25 μm and 10 μm particle sizes as a function of the compressive stresses needed to consolidate the respective powders. The compressive stresses were taken from Ferreira and Meyers' calculation [4], at a distention corresponding to an initial density of 65% of the theoretical density (this is a typical value for powders). Tensile stresses due to reflections are always present in shock consolidation systems. In well designed systems a significant portion of the tensile stresses is trapped. When the tensile stresses exceed the

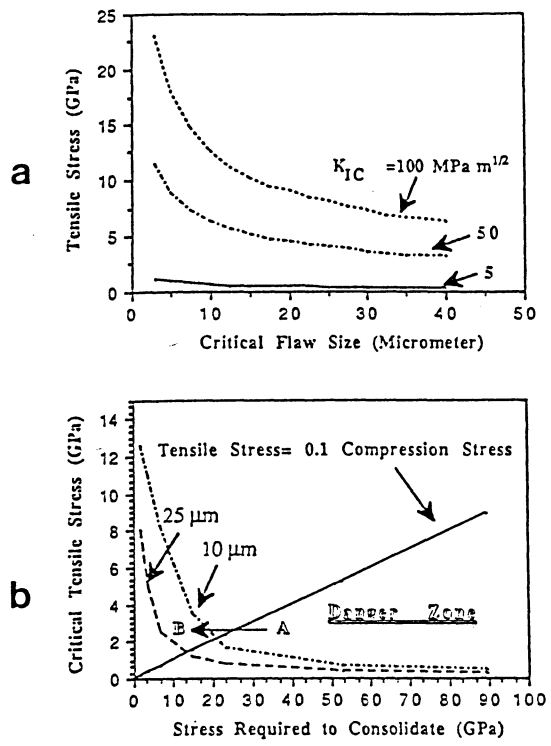

Figure 7. (a) Critical flaw size as a function of tensile stress; (b) variation of critical tensile stress for 10 and 25 μm flaw activation.

critical tensile stresses for the specific material, failure occurs; this is shown in Figure 7(b) in a schematic fashion. A realistic line shows $\sigma_t = 0.1\sigma_c$, i.e., the tensile reflections have, at most, an amplitude of 10% of the compressive pulse. Thus, a "Danger Zone" is marked in the figure. By reducing the shock amplitude point [A] (corresponding to a hypothetical material) is changed to [B]. Thus, there are three approaches to be implemented for improved shock consolidation. Reduction of tensile stresses requires systems where the design geometry is optimized. Shock energy can be reduced by thermal or chemical energy in an effort to improve compact quality. The reduction in powder size (e.g., nanocrystalline), reducing a, the flaw size, is the third approach.

REFERENCES

1. W.H. Gourdin, *J. Appl. Phys*, 55, p.55 (1984).
2. R.B. Schwarz, P. Kasiraj, T. Vreeland Jr., and T.J. Ahrens, *Acta Metall.*, 32, p. 1243 (1984).
3. V.F. Nesterenko, Proc. Novosibirsk-Conference on Dynamic Compaction, (1988) p. 100.
4. A. Ferreira and M.A. Meyers, in "*Shock Wave and High Strain Rate Phenomena in Materials*," M. Dekker, 1992, p. 361.
5. D.J. Benson, An Analysis by Direct Numerical Simulation of the Effects of Particle Morphology on the Shock Compaction of Copper Powder, UCSD, 1993.
6. R.L. Williamson, *J. Appl. Phys.*, 68, p. 1287 (1990).
7. V.F. Lotrich, T. Akashi, and A.B. Sawaoka, in *Metallurgical Applications of Shock Wave and High-Strain-Rate Phenomena*, eds. L.E. Murr, K.P. Staudhammer, and M.A. Meyers, M. Dekker, 1986, p. 277.
8. T. Akashi and A.B. Sawaoka, U.S. Patent 4.655.830 (1987).
9. S.S. Shang, Ph.D. Dissertation, UCSD, 1992.
10. A.S. Helle, K.E. Easterling and M.F. Ashby, *Acta Metall.*, 33, p. 2163 (1985).
11. D.J. Benson, *Comp. Meth. in Appl. Mech. and Eng.*, 99, p. 235 (1992).
12. D.J. Steinberg and M.W. Guinan, A High Strain Rate Constitutive Model for Metals, Technical Report UCRL-80465, Lawrence Livermore National Laboratory, 1978.